

Characteristics of Smith-Purcell radiation in millimeter wavelength region

This content has been downloaded from IOPscience. Please scroll down to see the full text.

2016 J. Phys.: Conf. Ser. 732 012018

(<http://iopscience.iop.org/1742-6596/732/1/012018>)

View [the table of contents for this issue](#), or go to the [journal homepage](#) for more

Download details:

IP Address: 134.219.215.122

This content was downloaded on 09/08/2016 at 07:42

Please note that [terms and conditions apply](#).

Characteristics of Smith-Purcell radiation in millimeter wavelength region

G A Naumenko¹, A P Potylitsyn¹, P Karataev³, V Bleko², L G Sukhikh¹,
M V Shevelev¹, Yu Popov¹

¹Tomsk Polytechnic University, Lenina Ave. 2a, Tomsk, Russia

²RASA Center in Tomsk, Tomsk Polytechnic University, Lenina Ave. 2a,
Tomsk, Russia

³John Adams Institute at Royal Holloway, University of London, Egham, Surrey, TW20 0EX,
United Kingdom

E-mail: naumenko@tpu.ru

Abstract. Investigations of the Smith-Purcell radiation (SPR) were began with non-relativistic electron beams with some unexpected experimental results. Further the experimental investigations were performed with relativistic electron beams for application to beam diagnostics. Large discrepancy between different theoretical models significantly increases the role of experimental studies of this phenomenon. In this report we present some problems and features of experimental investigations of SPR in millimeter wavelength region. The problems of prewave zone and coherent effects are considered. The shadowing effect, focusing of radiation using a parabolic SPR target and effect of inclination of target strips were investigated with moderately relativistic electron beam.

1. Introduction

The incoherent SPR arising when a charged particle passes over a periodic structure was observed for the first time in 1953 [1]. In view of a target periodicity the SPR will be monochromatic, i.e., there exists a stiff correlation between its wavelengths and the direction of radiation (the so-called Smith-Purcell dispersion relationship from [1]):

$$\lambda = \frac{d}{k} \left(\frac{1}{\beta} - \cos \theta \right),$$

where λ is the radiation wavelength, k is the diffraction order, d is the target period, β is the electron speed to that of light ratio, and θ is the observation angle (figure 1). Figure 2 shows the dependence of relation λ / d on observation angle for different k and $\beta \approx 1$.

Very exotic results have been obtained in experiment [2]. In this work using the beam of electron microscope, the fourth order was observed in dependence of infrared radiation intensity on the beam current. Unfortunately this effect was not confirmed yet.

In recent experiments [3, 4], the possibility of creating a monochromatic radiation source of the THz range on the basis of the Smith-Purcell radiation (SPR) has been demonstrated. The SPR from low relativistic electrons is also used in orotrons. The dispersion relationship is very useful for using of a coherent SPR (CSPR) in non-invasive beam diagnostics, namely for bunch length measurements



[5]. For the non-relativistic electron energies ($E_e \leq 100$ keV), the approach developed by van den Berg [6, 7] ensures a reasonable agreement with experiment [8, 9].

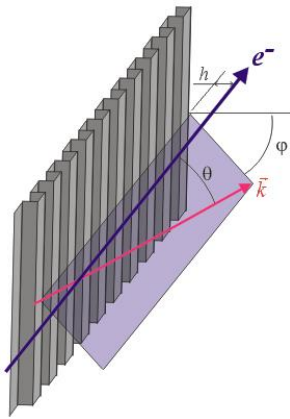


Figure 1. Designation of variables parameters.

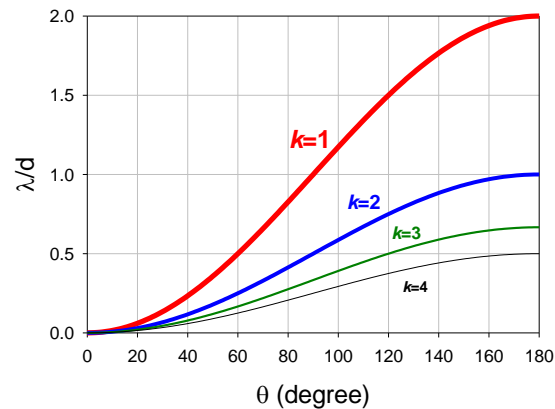


Figure 2. Dependence of relation λ/d on observation angle for different k .

In experiment [10], the possibility of applying the SPR of high relativistic electrons as a spontaneous radiation mechanism for a free-electron laser has been investigated. However until now no conventional model to calculate the characteristics of the SPR from high relativistic electrons is available.

In [11] the different models for SPR characteristics calculation were theoretically compared for high relativistic electrons:

- resonant diffraction radiation (RDR) model. This model is used for gratings consisting of infinitely thin perfect conducting strips separated by vacuum gaps, including inclined strips [12];
- surface current (SC) model (the SPR is considered as a radiation generated by the current induced by the field of a particle moving in vacuum on a perfect conducting periodic surface);
- Van den Berg's (VdB) model (applicable for volume gratings).

There was shown that the predictions of most models differ by approx. 2 orders of magnitude for the electron energy 20 MeV [13] and by several orders for the electron energies $E_e = 855$ MeV [14]. The available experimental results do not provide an ultimate conclusion on the validity of one of these models.

We would like in this paper to take attention on the some features which take place during the experimental investigations of SPR in millimeter and sub-millimeter wavelength region.

2. Prewave zone effect

This effect takes place at a small distance R between a target and detector. In this case a target size contribution distorts the angular distribution of radiation, which is usually considered theoretically in a far field zone. This is well-known effect for a transition radiation (TR) [15], that appears when $R \leq \gamma^2 \lambda$, where γ is the Lorenz-factor of electrons and λ is the investigated wavelength of TR. However, it is not obvious to the SPR. The detailed analysis of the prewave zone effect for SPR was done in [11]. We may show that this effect for transversal size of SPR target $H \geq \gamma \lambda$ appears when

$R \gg \frac{L^2 (1/\beta + \cos\theta)}{2d} + 2\gamma^2 d \cdot (1/\beta - \cos\theta)$, where L is a longitudinal size of target, d is period of target and $\beta = \sqrt{1 - 1/\gamma^2}$.

For example:

a) for $L = 200$ mm; $\gamma = 12$; $\theta = \pi/2$; $d = 12$ mm we obtain far field zone condition $R > 5$ m,

b) for $L = 20$ mm; $\gamma = 2000$; $\theta = \pi/2$; $d = 800$ nm (KEK ATF conditions, optical region) $R > 4$ m.

It is clear, that it is problem (sometimes impossible) to provide measurements in far field zone. To exclude the prewave zone effect a parabolic telescope (see figure 3) with detector placed in focus of parabolic mirror may be used for the spectral and angular distributions measurement. This method was proposed and tested in [16] and gives the same angular distribution as in the far field zone.

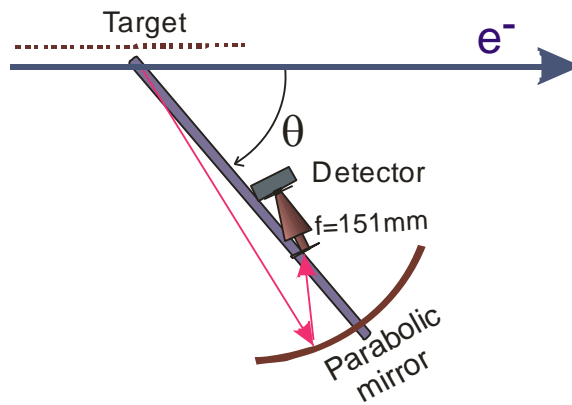


Figure 3. Scheme for suppression of the prewave zone effect.

3. Coherency factor

Another problem is the coherent effect of radiation of a bunched electron beam. The coherent radiation intensity of electron bunch may be presented as $W_{\text{coh}} \approx N_e \cdot f^2 \cdot W_{\text{incoh}}$. Here $N_e \gg 1$ is a bunch population, W_{incoh} is the incoherent radiation of electrons in bunch and f is the geometrical form-factor of a bunch.

For SPR the longitudinal form-factor f_{\parallel} gives contribution only, if $\sigma_{\perp} \ll \frac{\gamma\lambda}{2\pi} e^{\frac{2\pi h}{\gamma\lambda}}$ (see [31]), where σ_{\perp} defines a transversal size of bunch and h is impact-parameter. For Gaussian

approximation of longitudinal distribution of electron in bunch $f = f_{\parallel} = e^{-2\left(\frac{\pi\sigma_{\parallel}}{\beta\lambda}\right)^2}$, where σ_{\parallel} defines a longitudinal size of bunch.

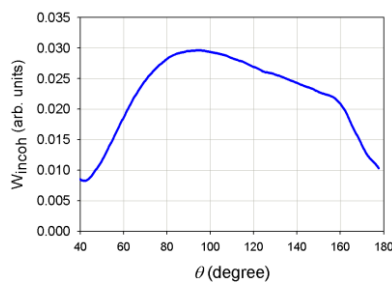


Figure 4. SPR polar distributions, calculated using surface current model for incoherent radiation.

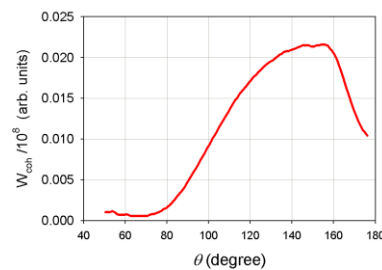


Figure 5. SPR polar distributions, calculated using surface current model for coherent radiation.

In figures 4 and 5 are presented the sample of SPR polar distributions, calculated using surface current model for incoherent and coherent radiation correspondently for next conditions:

$L = 160$ mm; $d = 8$ mm; strip width is equal 4 mm; impact-parameter $h = 10$ mm; $\sigma_{\parallel} = 2$ mm; $N_e = 10^8$.

So, form-factors are crucial in the formation of the spectral and angular characteristics of SPR.

4. Main SPR properties, observed using the electron beam of Tomsk Polytechnic University microtron

The experiment was performed on the extracted electron beam of microtron PTI TPU with the following parameters: electron energy – 6.1 MeV; macro-pulse duration – $4 \mu s$; the macro-pulse frequency $1 \sim 8$ Hz; the characteristic bunch length in the Gaussian approximation $\sigma_{\parallel} \approx 2$ mm; the bunch population $N_e = 10^8$, the number of bunches in macro-pulse – 10^4 , the cross-section of the extracted beam 4×2 mm², the angular divergence of the extracted beam – 0.08 rad. In figure 6 is presented the dependence of squared form-factor on the wavelength for these conditions.

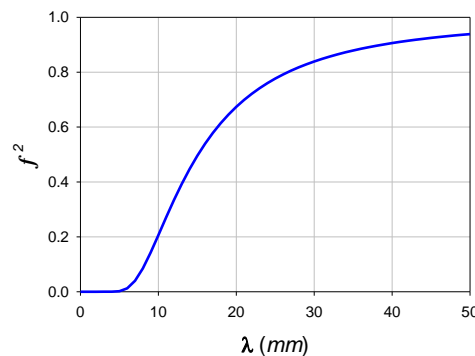


Figure 6. Dependence of squared form-factor on the wavelength.

Under these conditions for $\lambda > 9$ mm radiation of electron bunch is coherent. We may expect the radiation for $\lambda < 9$, but with a small intensity, which results large relative errors. Because of the coherency the radiation intensity is increased by N_e times (i.e., for the specified bunch population it is by 8 orders), making it available for the measurement using existing detectors operating at a room temperature.

For radiation registration, we used broadband detector DP-21M, manufactured in Semi-conductive Devices Research Institute (Tomsk, Russia) with parameters: efficiency in the wavelength region $\lambda = 3 \sim 16$ mm is estimated to be constant to a $\pm 15\%$ accuracy. The detector sensitivity is 0.3 V/mWatt. To suppress the accelerator RF system background the beyond cutoff waveguide with diameter 10 mm was mounted on the detector, which cuts a radiation having a wavelength $\lambda > 17$ mm. Thus, the spectral range of the measurement is $\lambda = 9 \sim 17$ mm.

The angular characteristics of the radiation were measured using the parabolic telescope (figure 3), which provides the measurements in terms of far field zone. The angular resolution of a telescope is 0.035 radians.

4.1. Comparison of different theoretical models of SPR

There are few theoretical models for calculate the SPR characteristics for the different grating profiles. We consider here three models: van den Berg's model (vDB) [6] (applicable for volume gratings), surface current model (SC) [17, 18] (the SPR is considered as a radiation generated by the current induced by the field of a particle moving in vacuum on a perfect conducting periodic surface), and resonant diffraction radiation model (RDR) [19] (for gratings consisting of infinitely thin perfect conducting strips separated by vacuum gaps). For comparison we use calculations and experimental

results from [20] (figure 7). We can see in figure 7 a large discrepancy between radiation yields obtained using these three models. Comparing the absolute experimental data with the theoretical predictions [20] ascertain that the RDR and SC models.

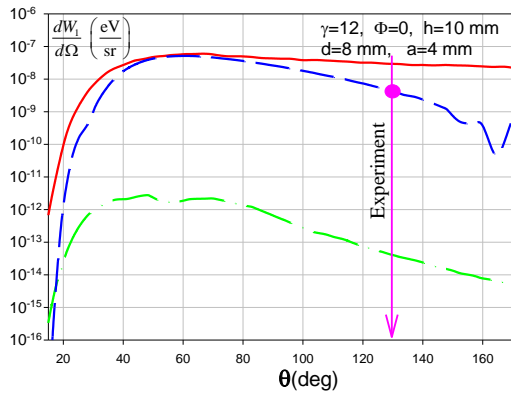


Figure 7. Angular distribution of the SPR intensity for a flat grating according to the RDR model (solid line), surface current model (a dashed curve) and for van den Berg's model (dash-dotted line). The point is the absolute experimental measurement

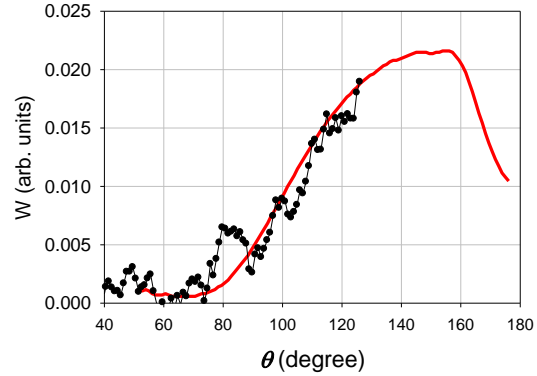


Figure 8. Polar angular distribution of measured coherent SPR. Dotted line is the experimental results. Solid line is calculation for far field zone using surface current model, normalized on the experimental results.

4.2. Angular dependence of coherent SPR

The polar angular distribution of measured coherent SPR (CSPR) from the flat target with parameters: $L = 200$ mm, $d = 12$ mm, strip width – 6 mm, impact-parameter $h = 10$ mm, is shown in figure 8. Solid line depicts the calculation of CSPR intensity normalized on the experimental results, for far field zone using surface current model for bunch length $\sigma_{||} \approx 2$ mm and for the same target parameters.

4.3. SPR focusing

Here we describe the possibility of CSPR focusing using a parabolic grating (figure 9). In this case we can obtain the focusing effect in a pre-wave zone without additional optic devices.

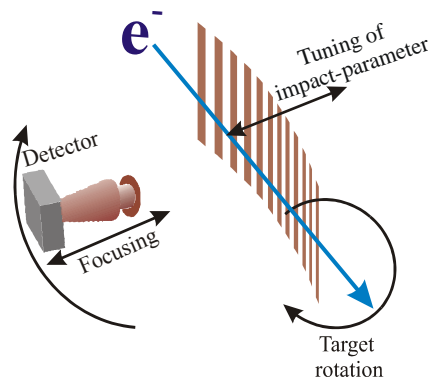


Figure 9. Scheme of CSPR focusing using a parabolic grating

In figure 10 is shown the dependence of radiation intensity on the distance between target and detector where we can see the maximum of radiation intensity in the focus of parabola. The comparison of

measured azimuthally orientation distributions of CSPR yield from polar-focusing (red curve) and flat (blue curve) gratings in corresponding conditions is shown in figure 11.

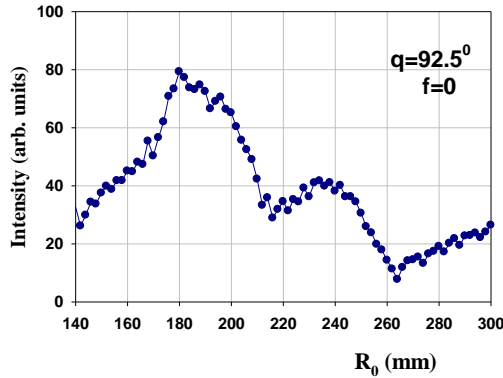


Figure 10. Experimentally measured distribution of CSPR yield vs. distance from the polar-focusing grating to detector.

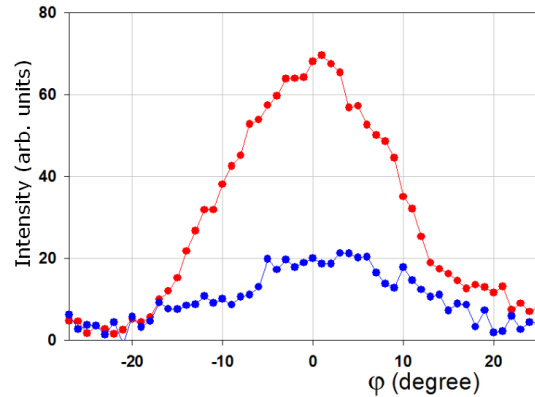


Figure 11. The comparison of experimentally measured azimuthally (at angle φ) orientation distributions of CSPR yield from polar-focusing (red curve) and flat (blue curve) gratings in corresponding conditions.

Here we can see that the focusing effect is limited due to increase of the impact-parameter in the center of parabolic target.

4.4. Shadowing effect in SPR

The shadowing of electron electromagnetic field in case of diffraction and transition radiation was considered theoretically and experimentally in number of papers [21] – [25]. In Pseudo-photon approach for ultra-relativistic electron the properties of electron field are very close to the properties of real photons. There is a region downstream to a conductive or absorbing screen where the Coulomb field is partly missing. In terms of paper [22] this effect is named “shadow effect”, and the term "semi-bare electron" has been introduced in [26, 27] to describe the similar effect in the framework of quantum electrodynamics for an electron scattered at a large angle.

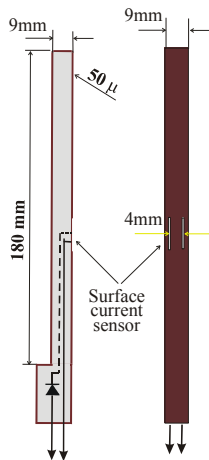


Figure 12. Active strip with surface current sensor.

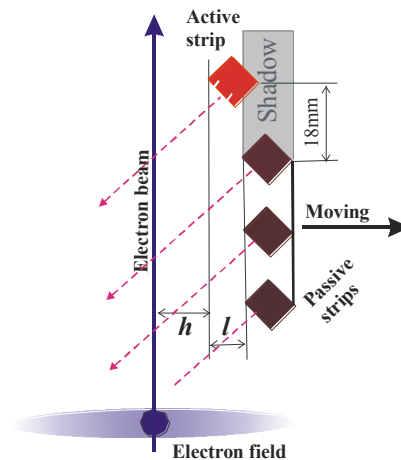


Figure 13. Scheme of shadowing measurements.

In [22] the shadowing effect for a Smith-Purcell radiation (SPR) was predicted by Prof. X. Artru. We apply in [28] the well-known technique, which is used in strip-line beam position monitors [29]. This sensor registered a surface current component perpendicular to the slit (see figure 12). The sensor was inserted in the element typical for a SPR target element (active element).

To be sure that we measure the concerned amount, we had measured the dependence of the surface current on impact-parameter (dots in figure 14). The solid line in figure 14 is the fit to experimental data.

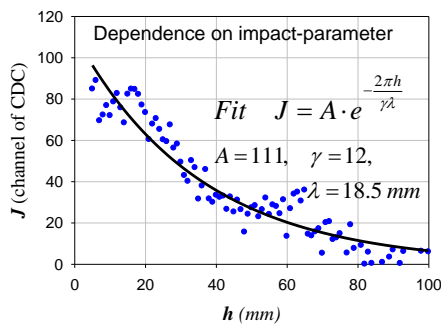


Figure 14. Dependence on impact-parameter. Dots are the experimental points. Solid line is fit shown approximation.

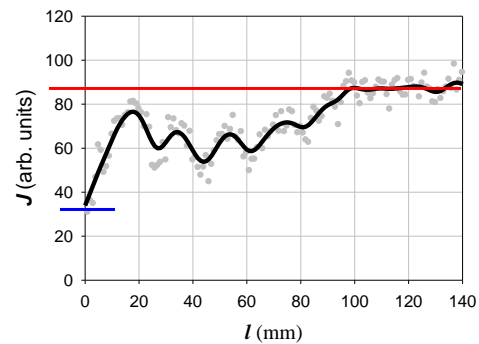


Figure 15. Dependence of surface current on the surface of active element on impact-parameter of the passive elements.

For measuring the shadowing effect we had inserted three grating elements of the same geometry but without a sensor (passive elements) upstream to the active element (see figure 13). In this geometry the active grating element corresponds to the fourth element in SPR target with width of element 9 mm and period 18 mm. The dependence of surface current on the surface of active element on impact-parameter of the passive elements (figure 15) shows the shadowing effect is equal 64%. This effect is of considerable importance to be taken into account in a calculation of SPR.

4.5. Effect of SPR target inclination (conical effect)

This item is devoted to the so named conical effect, predicted theoretically in [30]. According this prediction the maximum of azimuthal (φ) and polar (θ) distribution of SPR depends on an inclination angle ψ of a SPR target in respect to an electron beam (figure 16).

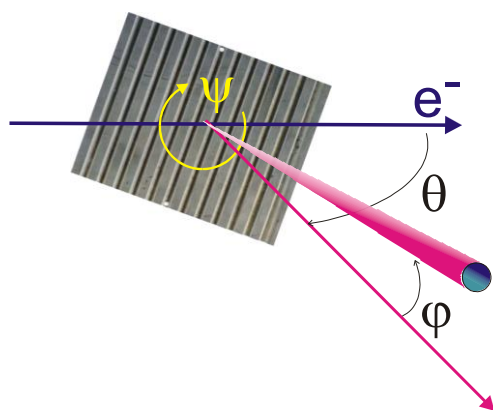


Figure 16. Designation of variable parameters in the experiment.

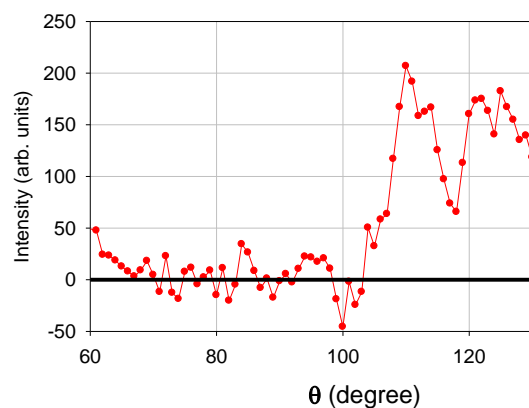


Figure 17. The dependence of radiation intensity on the polar angle θ for $\varphi = 0$ and $\psi = 0$.

The dependence of radiation intensity on the polar angle θ for $\varphi=0$ and $\psi=0$ in designation of variable parameters in the experiment shown in figure 16 is shown in figure 17. In figure 18 are shown the azimuthal dependences of SPR intensity in the point $\theta=110^\circ$ for $\psi=0$, $\psi=3^\circ$ and $\psi=5^\circ$. The dependences are normalized on the maximum of radiation intensity.

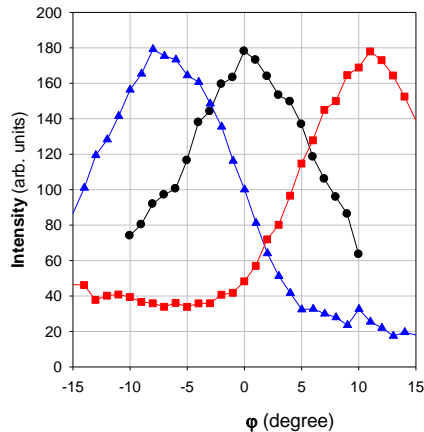


Figure 18. Azimuthal dependences of SPR intensity for $\psi=0$ (circles), $\psi=3^\circ$ (triangles), $\psi=5^\circ$ (squares).

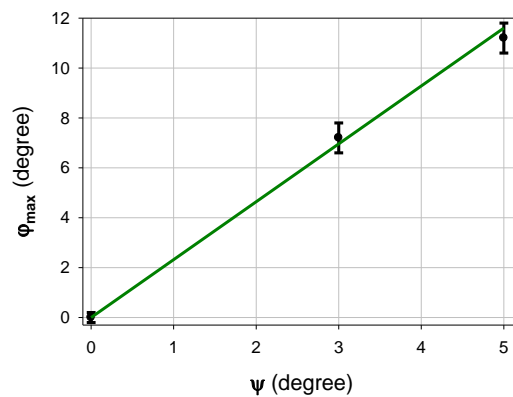


Figure 19. Dependence of maximum position φ_{\max} on the orientation angle ψ of the target in respect to the beam direction. Line is the linear fit.

Using these results we can build the dependence of maximum position φ_{\max} on the orientation angle ψ of the target in respect to the beam direction (figure 19). In figure 19 we can see the strong dependence of angular peak position φ_{\max} on the orientation angle ψ of the target.

The effect of azimuthal inclination of radiation due to rotation of target may be used for direct noninvasive measurement of a beam direction at a given point of the beam trajectory.

5. Conclusion

The existing theoretical calculations of SPR properties show the large discrepancy between them and can be used for estimations only (except kinematical calculations), and should be tested experimentally. Prewave zone effect should be estimated, for each geometry in angular and spectral measurements. The coherent properties of radiation of a bunched electron beam may be used for bunch length measurement. A parabolic SPR target may be used for the focusing of SPR. The shadowing effect should be taken into account in theoretical estimations. The effect of azimuthal inclination of radiation due to rotation of target may be used for direct noninvasive measurement of a beam direction.

Acknowledgment

This work was supported by grant RFBR 15-52-50028

References

- [1] Lampel M C 1999 *Advanced Accelerator Concepts: Eighth Workshop* (AIP, New York)
- [2] Bakhtyari A, Walsh J E, and Brownell J H 2002 *Phys. Rev. E* **65** 066503
- [3] Shibata Y, Hasebe S, Kimihiro Ishi K *et al* 1998 *Phys. Rev. E* **57** 1061
- [4] Korbly S E, Kesar A S, Sirigiri J R and Temkin R J 2005 *Phys. Rev. Letters* **94** 054803
- [5] Doucas G, Blackmore V, Ottewell B and Perry C 2006 *Phys. Rev. ST AB* **9** 092801

- [6] Van den Berg P M 1973 *J. Opt. Soc. Am.* **63** 1588
- [7] Van den Berg P M 1973 *J. Opt. Soc. Am.* **63** 689
- [8] Gover A, Dvorkis P and Elisha U 1984 *J. Opt. Soc. Am. B* **1** 723
- [9] Adischev Y N, Vukolov A V, Karlovets D V, Potylitsyn A P and Kube G 2005 *JETP Letters* **82** 174
- [10] Backe H, Lauth W, Mannweiler H *et al* 2006 *NATO Workshop 'Advanced Radiation Sources and Applications'* (Springer, New York) 267
- [11] Karlovets D V and Potylitsyn A P 2006 *Phys. Rev. ST AB* **9** 080701
- [12] Potylitsyn A, Karataev P, Naumenko G 2000 *Phys. Rev. E* **61** (6) 7039
- [13] Kesar A S 2005 *Phys. Rev. ST Accel. Beams* **8** 072801
- [14] Kube G, Backe H, Euteneuer H *et al* 2002 *Phys. Rev. E* **65** 056501
- [15] Verzilov V A 2000 *Phys. Lett. A* **273** 135
- [16] Kalinin B N, Naumenko G A, Potylitsyn A P *et al* 2006 *JETP Letters* **84** 3 110
- [17] Brownell J H, Walsh J and Doucas G 1998 *Phys. Rev. E* **57** 1075
- [18] Brownell J H and Doucas G 2005 *Phys. Rev. ST Accel. Beams* **8** 091301
- [19] Potylitsyn A P 1998 *Nucl. Instrum. Methods Phys. Res. Sect. B* **145** 60
- [20] Naumenko G, Kalinin B, Saruev G *et al* 2007 *Proceedings of symposium FEL Novosibirsk Russia WEPPH055*
- [21] Naumenko G, Artru X, Potylitsyn A *et al* 2010 *Journal of Physics: Conference Series* **236** 012004
- [22] Artru X, Ray C 2007 *International Conference on Charged and Neutral Particles Channeling Phenomena II*, Proc. SPIE **6634**
- [23] Naumenko G A, Potylitsyn A P, Sukhikh L G *et al* 2009 *JETP Letters* **90** (2) 96
- [24] Naumenko G, Artru X, Potylitsyn A, Popov Yu and Sukhikh L 2010 *Proceedings of symposium "Charged and neutral particles channeling phenomena - Channeling 2008"* 511
- [25] Naumenko G, Potylitsyn A, Popov *et al* 2009 *ArXiv.org physics* arXiv:0901.2630
- [26] Feinberg E L 1979 *Sov. Phys. Uspekhi* **22** 479
- [27] Shul'ga N F and Syshchenko VV 2000 *Journal Physics of Atomic Nuclei* **63** 2018
- [28] Naumenko G A, Potylitsyn A P, Popov Yu A, Shevelev M V 2011 *Nuovo Cimento C* **35** 4 305
- [29] Sargsyan V 2004 *TESLA Report* **03**
- [30] Sergeeva D Yu, Tishchenko A A and Strikhanov M N 2015 *Phys. Rev. ST* **18** 052801
- [31] Naumenko G 2015 *Advanced Materials Research* **1084** 138